

# Properties and relationship between solar eruptive flares and Coronal Mass Ejections during rising phase of Solar Cycles 23 and 24

M. Syed Ibrahim<sup>1</sup>, A. Shanmugaraju<sup>1</sup>, Y. -J. Moon<sup>2</sup>, B. Vrsnak<sup>3</sup>, S. Umaphy<sup>4</sup>

<sup>1</sup>Department of Physics, Arul Anandhar College, Karumathur - 625514, Madurai, India.  
Email: pgphysicsibrahim@gmail.com, ashanmugaraju@gmail.com

<sup>2</sup>School of Space Research, Kyung Hee University, Yongin 446-701, Republic of Korea.  
Email: moonyj@khu.ac.kr

<sup>3</sup>Faculty of Geodesy, Hvar observatory, Zagreb, Croatia. Email: bvrsnak@gmail.com

<sup>4</sup>Department of Science & Humanities, Rathinam Institute of Technology, Coimbatore, India.  
Email: umaphymku@gmail.com

## Abstract

Statistical relationship between major flares and the associated CMEs during rising phases of Solar Cycles 23 and 24 are studied. Totally more than 6000 and 10000 CMEs were observed by SOHO/LASCO (Solar and Heliospheric Observatory/ Large Angle Spectrometric Coronagraph) during 23<sup>rd</sup> [May 1996 - June 2002] and 24<sup>th</sup> [December 2008 - December 2014] solar cycles, respectively. In particular, we studied the relationship between properties of flares and CMEs using the limb events (longitude 70°-85°) to avoid projection effects of CMEs and partial occultation of flares that occurred near 90°. After selecting a sample of limb flares, we used certain spatial and temporal constraints to find the flare-CME pairs. Using these constraints, we compiled 129 events in Solar Cycle 23 and 92 events in Solar Cycle 24. We compared the flare-CME relationship in the two solar cycles and no significant differences are found between the two cycles. We only found out that the CME mean width was slightly larger and the CME mean acceleration was slightly higher in cycle 24, and that there was somewhat a better relation between flare flux and CME deceleration in cycle 24 than in cycle 23.

**Key words:** Coronal Mass Ejection (CME), Flare

## 1. Introduction

Coronal mass ejections (CMEs) are powerful solar eruptive events that launch large amounts of plasma and magnetic flux from the solar atmosphere into the heliosphere (e.g., Manoharan et al., 2004 and Manoharan, 2006). These sudden "explosions" are frequently associated with sudden enhancements of the emission in the H-alpha, radio, EUV, and X-ray wavelengths, called solar flares (Joshi et al., 2007; 2009; 2011; 2012). On the other hand, a significant fraction of flares is not associated with CMEs; typically the association rate increases with the intensity of flares (Gosling et al., 1976; MacQueen and Fisher, 1983; Harrison, 1995; Sheeley et al., 1999; Andrews and Howard, 2001). The most powerful events usually occur in regions of strong complex magnetic field that becomes unstable and erupts

1  
2  
3  
4  
5  
6  
7  
8  
9  
violently into the interplanetary medium, resulting also in rapid heating of chromospheric and  
coronal plasma (Kahler, 1992). Zhang et al. (2001; 2006) and Shanmugaraju et al. (2003),  
Vrsnak et al. (2004) and Maricic et al. (2007) reported the coincidence between the main  
acceleration stage of CMEs and flare impulsive phase, whereas Vrsnak et al. (2007) found  
that, statistically, the magnitude of CME acceleration depends on the impulsiveness of the  
associated solar flare.

10  
11  
12  
13  
14  
15  
16  
17  
18  
19  
20  
21  
22  
23  
24  
25  
26  
27  
28  
29  
30  
31  
32  
33  
The relationship between CMEs and flares was investigated by many authors in the  
past (e.g. Munro et al., 1979; Kahler 1992; Harrison, 1995; Hundhausen, 1997) up to present  
days (Mahrous et al., 2009; Jain et al. 2010; Youssef, 2012; Salas-Matamoros and Klein,  
2015, and references therein). Mahrous et al. (2009) analysed the flare-CME association  
during the Solar Cycle 23. Initially, they took 224 flare-CME events and found correlation  
between the CME energy and flare flux, characterized by a correlation coefficient of  $R=0.52$ .  
After that they reduced the sample to 55 flare-CME events that satisfied a temporal  
constraint, which increased the correlation coefficient to  $R=0.61$ . Finally, they took only 41  
flare-CME pairs that satisfied the spatial and temporal conditions, and the correlation  
increased up to 76%. Using a set of 26 events in cycle 23, Jain et al. (2010) studied the  
relationship between the velocity of CMEs and the plasma temperature of the associated X-  
ray solar flares and found a positive correlation between the CME velocity and plasma  
temperature, characterized by a correlation coefficient of  $R = 0.82$ .

34  
35  
36  
37  
38  
39  
40  
41  
42  
43  
44  
45  
46  
47  
48  
49  
50  
51  
52  
53  
54  
55  
56  
57  
Youssef (2012) examined the relationship between the CMEs and flares during the  
period of 1996-2010. Initially, a set of 776 flare-CME events was studied and a correlation of  
 $R=0.38$  between flare flux and CME energy was found. After using the temporal and spatial  
constraints, the correlation coefficient increased up to  $R = 0.65$ . Salas-Matamoros and Klein  
(2015) found the relationship between the CME and flares using a set of 77 flare-CME pairs  
observed in the period 1996 - 2008. They excluded events with the central position angle  
below  $\pm 60^\circ$ , limited the CME width to the range  $60^\circ$ - $120^\circ$  and excluded CMEs with speeds  
below 100 km/s. They found a correlation between the CME speed and the soft X-ray flux  
and fluence of the associated flares, characterized by  $R=0.48$  for flare flux and 0.58 for  
fluence. They also performed the analysis separately for three types of flares, considering the  
flare time profiles: (i) simple bursts showing a single peak, (ii) events constituted of a  
superposition of two different soft X-ray bursts and (iii) a bursts characterized by a very  
complex time profile.

58  
59  
60  
61  
62  
63  
64  
65  
Shanmugaraju et al. (2011) compared the relationship between physical properties of  
CMEs and flares associated with type II radio bursts with those without type II bursts. They

1 analysed a sample of 290 events during the period January 1997 to December 2000. In this  
2 study, a better CME-flare relationship was found for the events associated with type II bursts.  
3 Bak-Steslicka et al., (2013) investigated 24 CME-associated long-duration flares and found a  
4 positive correlation between the CME speed and the flare flux of  $R = 0.77$ .

5 Thus, the flare-CME relationship is not completely, since the results depend very  
6 much on the applied the selection criteria and the employed statistical procedure.  
7 Furthermore, the difference between Solar Cycles 23 and 24 has been recently noted by  
8 Gopalswamy et al., (2015a). They reported that although the sunspot number in cycle 24 has  
9 dropped by ~40%; the number of halo CMEs in cycle 24 was nearly the same as in cycle 23.  
10 They also found that the distribution of halo-CME source locations is different in the cycle  
11 24. Prasanna Subramanian and Shanmugaraju (2016) examined intense flares (>M5.0 class)  
12 in cycle 24 and reported that the number of intense flares reduced by ~34 % from that in  
13 cycle 23. Hence, a comparison of the flare-CME relationship in cycles 23 and 24 is an  
14 important objective to be studied.

15 In this paper, we compared the basic properties of CMEs and flares, and the  
16 characteristics of the flare-CME relationship during the rising phase of these two solar cycles.  
17 We focus on limb events that originated in regions  $70^{\circ}$ - $85^{\circ}$  from the disc centre. We analyse a  
18 sample of 129 flare-CME pairs observed in Solar Cycle 23 and 92 flare-CME pairs from  
19 Solar Cycle 24, using these two samples, we study characteristics and relationships between  
20 CMEs and flares to investigate possible differences between Solar Cycles 23 and 24,  
21 considering all events, as well as M+X class flares separately. The number of M+X events  
22 was 40 and 31 in Solar Cycles 23 and 24, respectively. Data analysis is presented in section 2,  
23 and results and discussion are presented in section 3. Conclusions are drawn in section 4.

## 2. Data Analysis

24 During the rising phase of Solar Cycles 23 [1996 (May) - 2002 (June)] and 24 [2008  
25 (December) - 2014 (December)], more than 6000 and 10000 CMEs was observed by  
26 SOHO/LASCO (Solar and Heliospheric Observatory/ Large Angle Spectrometric  
27 Coronagraph) spacecraft. We selected the events observed during the period of 73 months (as  
28 considered by Gopalswamy et al., 2015b) to investigate the limb flares and CMEs. Within 73  
29 months, data for 4 months are excluded because of missing SOHO/LASCO data. The CME  
30 data are taken from the SOHO/LASCO online catalogue of CMEs  
31 ([http://cdaw.gsfc.nasa.gov/CME\\_list/index.html](http://cdaw.gsfc.nasa.gov/CME_list/index.html)). The soft X-ray (SXR) flare burst data are  
32 gathered from Geostationary Environmental satellite (GOES)  
33 (<http://www.ngdc.noaa.gov/stp/space-weather/solar-data/solar-features/solar-flares/x->

1 rays/goes/xrs/). From the complete sample of events, we selected limb events, located within  
2 70° - 85° from the disc centre, since the projection effect on the properties of limb CMEs is  
3 significantly reduced compared to the on-disc events. We excluded the events that occurred  
4 beyond 85° to avoid the events too close to the limb, carrying the risk that some are partly  
5 occulted and their SXR flux being reduced. From the complete list of events, we associate the  
6 flares and CMEs using several temporal and spatial constraints. First, the time difference  
7 between the flare start and CME onset was constrained to a time window of  $\pm 90$  minutes.  
8 Here, CME onset means the initiation time of the CME, i.e., the back-extrapolated onset time  
9 based on the LASCO C2 height-time data. This CME onset time was taken from the LASCO  
10 CME catalogue, where two onset times are reported for each observed CME (onset 1 and  
11 onset 2 using linear and quadratic fits, respectively). In the following, we employ the one  
12 based on the linear fit on the height time data (Gopalswamy et al., 2009). Also, we used the  
13 linear speed and angular width for CMEs as given in the LASCO catalogue, and used GOES  
14 SXR peak flux values for flares. It should be noted that in the catalogue, the CME velocity is  
15 determined for the fastest structural element of the CME signature. Since in the case of a fast  
16 CME a shock may be observed already in the LASCO field-of-view, this will be the velocity  
17 of the shock in such CMEs, which may significantly differ from the velocity of the CME  
18 body (piston) generating it (Gopalswamy et al., 2001; Shanmugaraju and Lawrance 2015).  
19 On the other hand, for slow CMEs without shocks, measured velocity is that of the CME  
20 body. Similarly, for fast CMEs, the CME angular size is measured taking into account the  
21 extent of a shock. In the case of slow CMEs, the size is measured taking into account only the  
22 CME body. These effects have a tendency to increase a scatter of data-points of points in the  
23 correlation plots. According to the spatial criterion, the CMEs should have been ejected from  
24 the same quadrant where the flares occurred. Furthermore, we used the EIT (Extreme Ultra-  
25 Violet Imaging Telescope) and SDO (Solar Dynamic Observatory) observations to check  
26 whether or not the flare and the CME originated from the same active region to avoid the  
27 back-sided events.

28  
29  
30  
31  
32  
33  
34  
35  
36  
37  
38  
39  
40  
41  
42  
43  
44  
45  
46  
47 Using the above mentioned criteria, we selected 129 events in Solar Cycle 23 and 92  
48 events in Solar Cycle 24. In both the Solar Cycles 23 and 24, locations of flares were  
49 identified using H-alpha optical observations. We took the flare location directly from the  
50 GOES catalogue. In this sample, 286 events are the limb flares located within 70° and 85°  
51 from the disc centre. From these 286 flares, 92 flare - CME pairs are selected (remaining  
52 flares did not satisfied the described selection criteria). Similarly, in the 23<sup>rd</sup> solar cycle,  
53 locations of more than six thousand flares are identified. From these flares, we filtered out the  
54 non-limb events and found the flare-associated CMEs using temporal and spatial conditions.

Finally, we got 129 flare - CME pairs in Solar Cycle 23. We note that during the period of Solar Cycle 23 (1996 May to 2002 June) LASC0 observed ~6000 CMEs (CME detection was very poor in the year 1996 and 1997). LASC0 observed ~10000 CMEs during the rising period of Solar Cycle 24 (2008-2014). On the other hand, GOES reported nearly ~7000 flares in Solar Cycle 23 and nearly ~3000 flares in the rising phase of Solar Cycle 24. From these flare observations, only flares with identified locations are taken into the account.

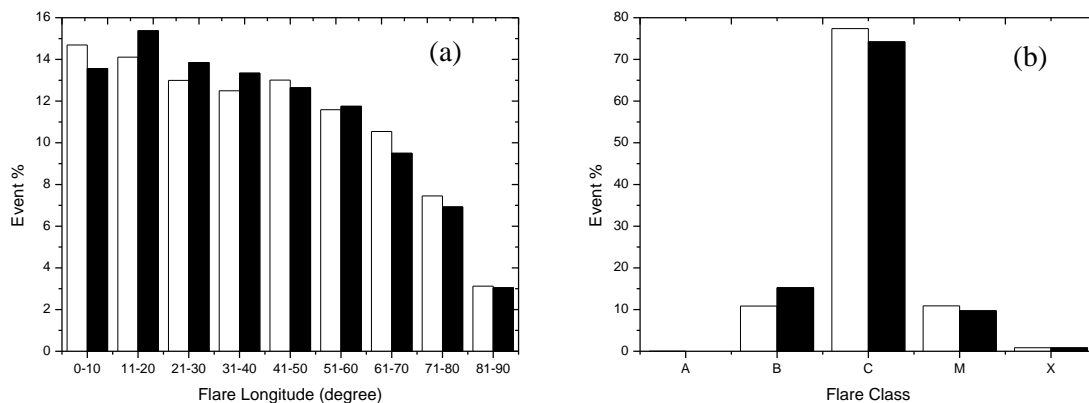


Fig. 1. Distribution of (a) Flare longitude; (b) Flare class (for all the flares). White and dark bars correspond to 23<sup>rd</sup> and 24<sup>th</sup> solar cycle, respectively.

For the considered set of all flares in Solar Cycles 23 and 24, the frequency of flares in 10° longitudinal bins and frequency of flares class (A, B, C, M, and X) are drawn in the distribution diagram (Fig. 1). Fig. 1a shows that the distribution of all the flares in Solar Cycles 23 and 24, had nearly equal percentage of limb flares, the percentage decreasing from centre to the limb. The distribution of flare classes, shown in Fig. 1b, shows that ~75% of flares are of class C in both solar cycles, whereas the percentage of A-class flare is very low. A lower percentage of flares at larger longitudes is similar to the results obtained by Conway and Matthews (2003), who used X-ray and H-alpha flares, but it is quite different from a more uniform distribution of RHESSI micro-flares reported by Christe et al. (2008)

### 3. Results

#### 3.1. CME and Flare properties

The distribution of CME and flare parameters for the both analysed periods are shown in Figs. 2 and 3, respectively. In Fig. 2a, it can be noted that the distribution of CME speed is similar in both cycles, except that cycle 24 has somewhat larger fraction of fast CMEs. Similarly, Fig. 2b, shows that there was more wider CMEs in cycle 24 than in cycle 23. In Fig. 2c a distribution of accelerations is presented, showing that there was somewhat larger

fraction of decelerating CMEs in the Solar Cycle 24 than in cycle 23. The mean and median values in CME properties are found to be nearly same in both the cycles (shown in Table 1).

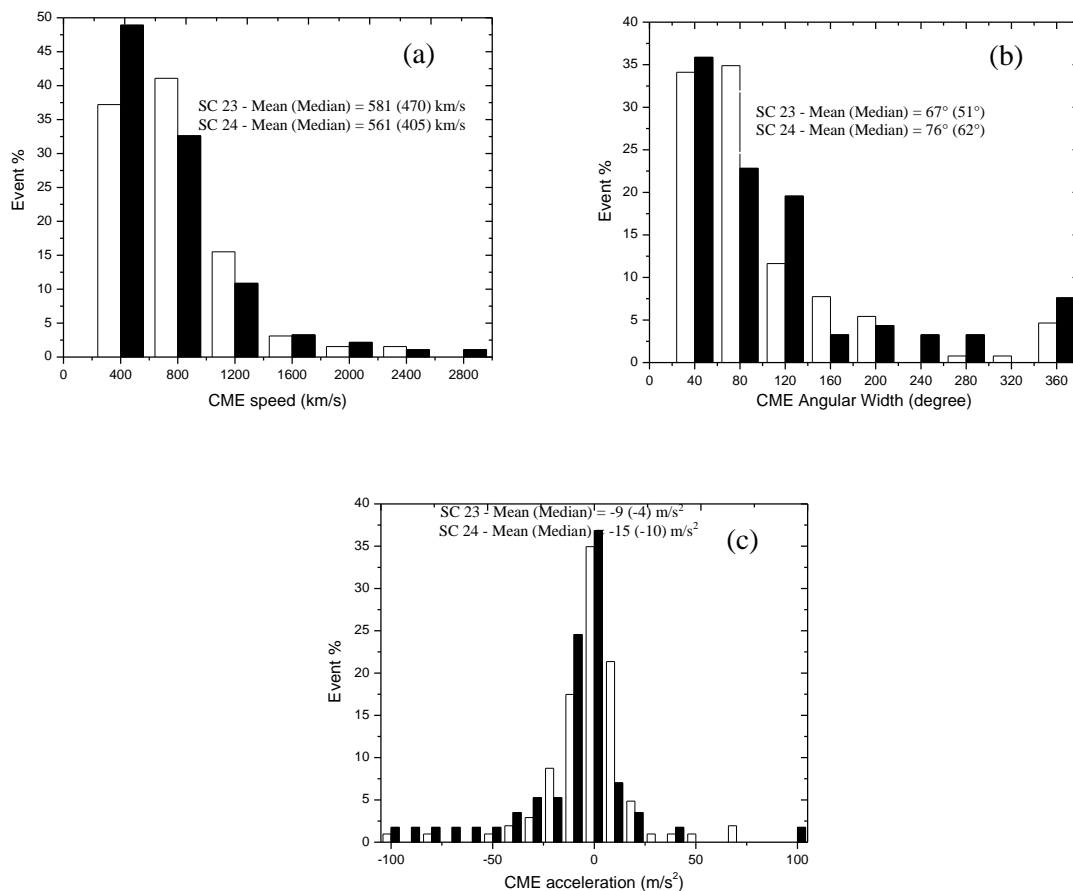


Fig. 2. Comparison of the 23<sup>rd</sup> and 24<sup>th</sup> solar cycle (white and dark bars, respectively): (a) Distribution of CME speed, (b) Distribution of CME angular width, (c) Distribution of CME acceleration/deceleration, (Solar Cycle 24: CME acceleration/deceleration values are available for 103 events. Solar Cycle 23: CME acceleration/deceleration available for 57 events).

Similarly, Fig. 3 shows nearly same distribution pattern and mean/median values of the flare rise time, duration and flare class for both the solar cycles. Flare rise time represents the difference between the SXR-flare start and flare peak time. The flare duration is estimated using the difference between the flare start and end times. Fig. 3d presented the SXR observation for X1.0 flare observed on 2002 August 3, showing the flare rising time (indicated by #1) and flare duration (indicated by #2). The starting time of an X-ray event is defined as the first minute, in a sequence of 4 minutes, of steep monotonic increase in 1.0 - 8.0 Å flux. The X-ray event maximum is determined as the minute when the X-ray flux reaches the peak value. The end time is the time when the flux level decays to a point halfway between the maximum flux and the pre-flare background level. Multiple flares are eliminated by checking the flare SXR profiles.

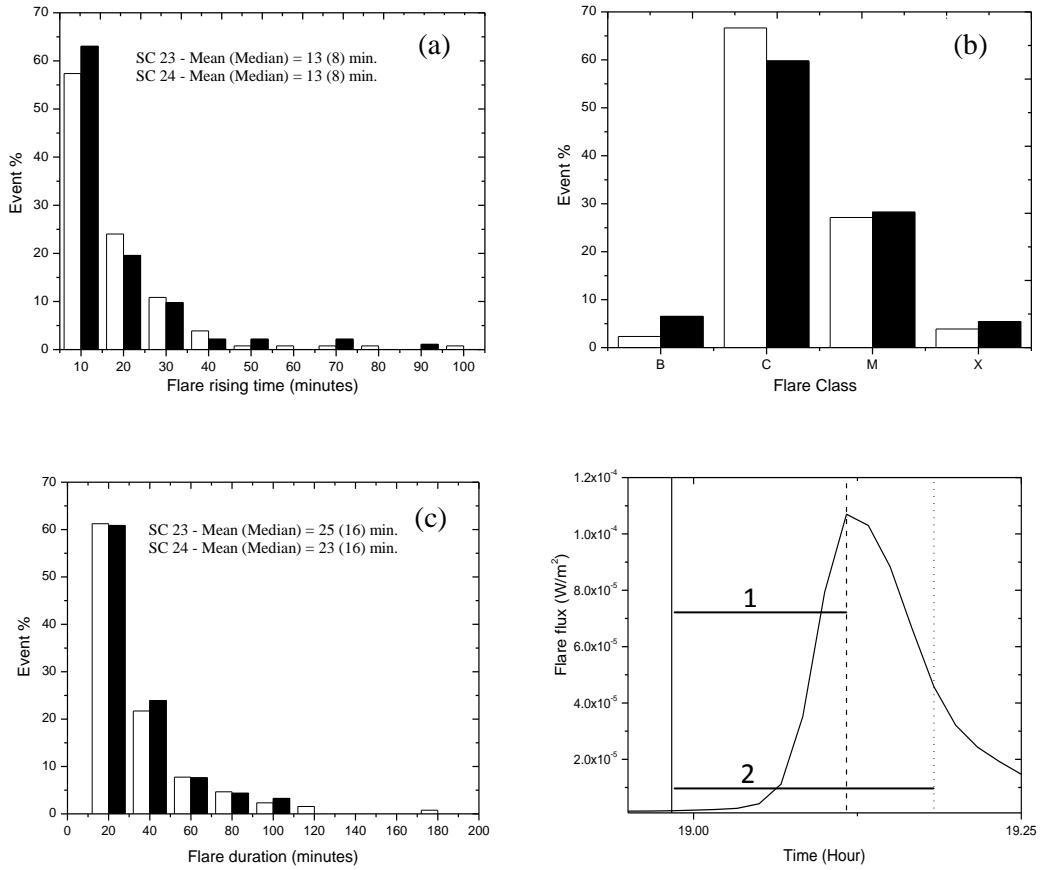


Fig. 3. Comparison of 23<sup>rd</sup> and 24<sup>th</sup> solar cycles; Distribution of (a) Flare rise time, (b) Flare class, (c) Flare duration, (d) X1.0 flare of 2002 August 3, as recorded in the X-ray range between 1.0 to 8.0 Å. The vertical solid, dashed and dotted black lines indicate the flare start (onset), peak and end times, respectively. The numbers 1 and 2 indicate the flare rising time and flare duration, respectively. White and dark bars indicate 23<sup>rd</sup> and 24<sup>th</sup> solar cycle events, respectively.

For the 23<sup>rd</sup> solar cycle, mean values of CME speed, width and acceleration are 581 km/s, 67° and -9 m/s<sup>2</sup> respectively. Mean values of flare rise time and duration are 13 and 25 minutes respectively. 69% of the CMEs are associated with B and C-class flares and 31% are associated with M+X class flares. Among 129 limb CMEs, 6 CMEs are full-halo events. For the 24<sup>th</sup> solar cycle, mean values of CME speed, width and acceleration are 561 km/s, 76° and -15 m/s<sup>2</sup> respectively. Mean values of flare rise time and duration are 13 and 23 minutes respectively. Among 92 limb CMEs in 24<sup>th</sup> solar cycle, 7 CMEs are full-halo events. The above results are summarized in Table 1 along with the standard deviation and median values. The mean, standard deviation and median values of CME width is calculated without taking into account halo CMEs. If an average width of CMEs is calculated including halo CMEs (width of 360°), the average is probably biased, because the assigned 360° width might be very different from the real opening angle of the CME. For acceleration study, we considered only the CMEs for which more than three height-time data points are measured. Statistical significance in the difference between the mean values of the two cycles is

obtained by employing the "t-test" (P-values are listed in last column of Table 1). If P-value is less than 0.05, then there is a statistically significant difference between two data sets.

Table 1 Statistical characteristic of CMEs and flares (values inside the brackets represent the standard deviation/median).

<b>CME parameters for all limb events</b>	<b>Cycle 23</b>	<b>Cycle 24</b>	<b>P- value</b>
Mean Speed	581 km/s (381/470 km/s)	561 km/s (452/405 km/s)	0.37
Mean Width	67° (54°/51°)	76° (61°/62°)	0.09
Mean Acceleration	-9 m/s <sup>2</sup> (42/-4 m/s <sup>2</sup> )	-15 m/s <sup>2</sup> (38/-10 m/s <sup>2</sup> )	0.17
<b>Flare parameters for all limb events</b>			
B and C class	69%	66%	--
M and X class	31%	34%	--
Mean Flare duration	25 min (25/16 min)	23 min (19/16 min)	0.23
Mean Rise time	13 min (14/8 min)	13 min (14/8 min)	0.39
Mean decay time	12 min ( 14/7 min)	11 min (9/8 min)	0.13
<b>CME parameters (M and X class flare associated)</b>	<b>Cycle 23</b>	<b>Cycle 24</b>	
Mean Speed	790 km/s (474/641 km/s)	905 km/s (587/710 km/s)	0.19
Mean Width	101° (69°/71°)	128° (76°/112°)	0.05
Mean Acceleration	-8 m/s <sup>2</sup> (15/-9 m/s <sup>2</sup> )	-16 m/s <sup>2</sup> (54/-8 m/s <sup>2</sup> )	0.23
<b>Flare parameters (M and X class)</b>			
Mean Flare duration	35 min (28/23 min)	32 min (22/25 min)	0.31
Mean Rise time	19 min (19/13 min)	18 min (13/14 min)	0.34
Mean decay time	16 min (15/9 min)	14 min (11/11 min)	0.31

After filtering out weak B and C SXR-class flares, we analysed in more detail statistical properties of the M+X class flares for the Solar Cycles 23 and 24. Though there are 40 and 31 M+X class events in cycles 23 and 24, the fraction of limb M+X class flares in cycles 23 and 24 are **quite** similar (31% and 34% respectively). The percentage of strong flares (M+X) is similar in both solar cycles. The statistical characteristics of M+X class events are also given in Table 1. There are slight differences between cycle 23 and 24 in the mean values of CME width and acceleration. However, according to the P-values the difference between Solar Cycles 23 and 24 is not statistically significant. While the mean CME widths of all limb events in cycle 23 and 24 are nearly the same (67° and 76°), the mean CME width of M+X class flare-associated events show slight difference (101° in cycle 23 against 128° in cycle 24). The reason may be attributed to the strength of flares and anomalous expansion. From the flare-CME relation studied by some authors (e.g., Harrison,



1995; Moon et al. 2002; Vrsnak et al., 2005; Prakash et al. 2014), it is known that the CMEs associated with stronger flares are wider than the CMEs associated with weaker flares. Anomalous expansion of CMEs of cycle 24 have been reported by Gopalswamy et al.(2015a) and was attributed to the reduced heliospheric pressure, since the effect of the aerodynamic drag should be more effective on wider CMEs Vrsnak et al. (2010). On the other hand, the previously mentioned similarity of the flare durations and rise times (for all limb events) between the two cycles is found for M+X class events too.

## 3.2. Correlation study

### 3.2.1. Limb events

Fig. 4 shows the relation between CME properties and flare flux for Solar Cycles 23 and 24 along with the correlation coefficient. Relationship between the flare flux and CME speed is compared for 23<sup>rd</sup> (Fig. 4a) and 24<sup>th</sup> (Fig. 4b) solar cycles. The graphs show that as the flare flux increases CME speed increases too. Here we used the Pearson product-moment correlation method to find the relationship between the flare-CME properties. The outcome is consistent with the literature demonstrating that CMEs associated with X-ray flares of high intensity are likely to be faster and wider (Gosling et al., 1976; Yashiro, 2009). It is also similar to the recent results of Salas- Matamoros and Klein (2015), who obtained a correlation of  $R = 0.48$  between CME speed and flare flux.

Figs. 4c and d show the relationship between the CME angular width and flare flux. In this particular analysis, we excluded the halo CMEs of angular width  $360^\circ$ . Similar correlations have already been reported between intensity of X-ray flares and energy of the associated CMEs (Hundhausen, 1997; Moon et al., 2002; Yashiro, 2009; Mahrous et al., 2009). In addition to these relations, we present in Figs. 4e and 4f the relationship between the CME deceleration and flare flux. Graphs show a better correlation for cycle 24 mainly because of three excess points associated with three X-class flares in cycle 24. The relations of **flare flux and CME speed/width** are similar in both the cycles. On the other hand, the relation of the flare flux and the CME deceleration seems to be somewhat different due to the X-class associated flares.

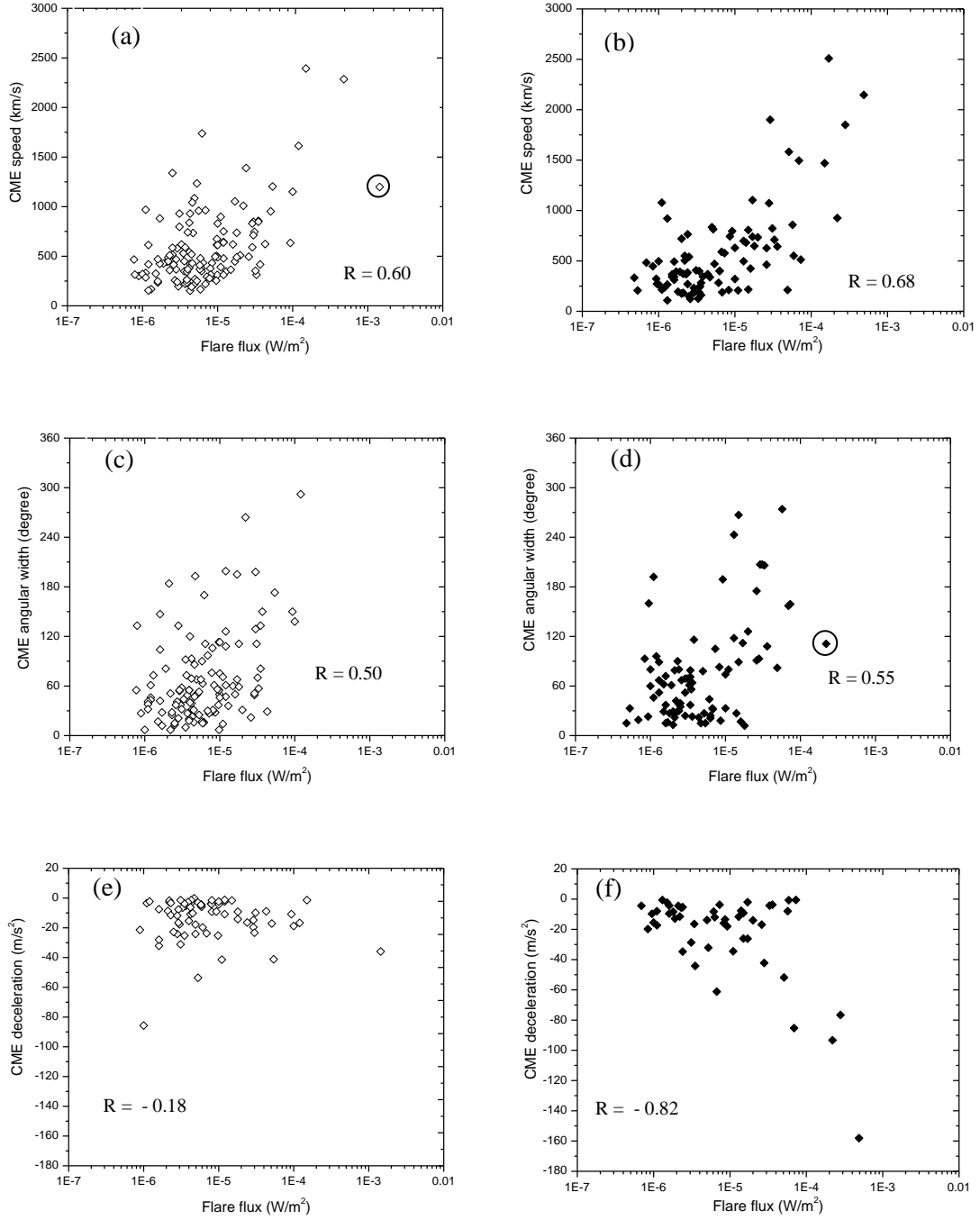


Fig. 4. (a) and (b) relationship between CME speed and flare flux. (c) and (d) relationship between CME angular width and flare flux. (e) and (f) relationship between CME deceleration and flare flux (left and right columns represent the 23<sup>rd</sup> and 24<sup>th</sup> solar cycles). The outlier point is not included in the correlation and it is indicated by the encircled symbol in (a) and (d).

During the considered period of 23<sup>rd</sup> and 24<sup>th</sup> solar cycles, 32 out of 129 CMEs and 7 out of 92 CMEs were accelerated, respectively, whereas the majority of CMEs were decelerated. Furthermore, the CME acceleration data points are distributed horizontally and show practically no correlation between the flare flux and CME acceleration. So, we excluded the accelerations part from this study in Fig. 4e and 4f. The inclusion of outlier events (encircled points) in Fig. 4a and 4d gives correlation coefficient of  $R = 0.34$  and  $R = 0.35$ , respectively.

### 3.2.2. M and X class limb events

1 For this set of events, the correlation plots presented in Fig. 5 show similar relations  
2 as those displayed in Fig. 4. The relations between flare flux and CME parameters are  
3 slightly better in cycle 24 than in cycle 23, mainly because of the presence of X-class flares.  
4 Besides, visually it appears that the correlation coefficients in Fig. 4f and in Fig. 5f are  
5 overrated: if one would remove 4-5 points corresponding to the largest flare-flux values, there  
6 is practically no correlation between the analysed parameters. For both the solar cycles, the  
7 relationship between the flare flux and the CME deceleration relationship becomes the same  
8 when we removed the few X-class flares in Figs. 4f and 5f.  
9  
10  
11  
12  
13  
14  
15

16 Bak-Steslicka et al. (2013) investigated the relationship between flare flux and CME  
17 speed for 24 slow and long duration events. Among the 24 events, 20 CMEs were associated  
18 with M+X class and their speeds were larger than 1000 km/s. They obtained a correlation  
19 between the CME speed and flare flux as  $R = 0.77$ . Also, they obtained the correlation  
20 between the flare flux and CME acceleration as  $R = 0.66$ . These results are similar to that in  
21 the present work for strong flares of cycle 24. Hence, the overall comparison between 23<sup>rd</sup>  
22 and 24<sup>th</sup> solar cycle shows that flare flux - CME relationship in 24<sup>th</sup> solar cycle is similar to  
23 that of 23<sup>rd</sup> solar cycle when the X-class flare events are removed. Recently, Compagnino et  
24 al. (2017) studied the relations between properties of flares and CMEs, using a sample of  
25 events that occurred in the period from 1997 July 31 to 2014 March 31 (period of solar cycles  
26 23 and 24). They used three different time windows (2 hour,  $\pm 1$  hour and  $\pm 30$  minutes) to  
27 identify the CME-flare pairs. In the present paper, the flare-CME association is checked  
28 using the temporal and spatial conditions for each flare-CME pair, checking that flares and  
29 CMEs originated from the same active region.  
30  
31  
32  
33  
34  
35  
36  
37  
38  
39  
40  
41  
42

43 Actually, it has been already reported by some authors (Hundhausen, 1997; Moon et  
44 al., 2002; Yashiro, 2009; Mahrous et al., 2009) that the relationship between the CME and  
45 flare energies depends on the strength of flares. That is, the relation is better in the case of  
46 more powerful flares. There were five X-class limb flares recorded in both cycles, but  
47 deceleration values are available only for four and three CMEs in cycles 23 and 24,  
48 respectively. A better correlation is obtained in 24<sup>th</sup> cycle, maybe because of the presence of  
49 high-energy flare-CME events in 24<sup>th</sup> solar cycle. Strong flares are associated with  
50 faster/wider CMEs which are prone to decelerate more strongly. This relationship obtained  
51 might be attributed to the physical effect. To confirm this, we separated from the set of all  
52 events those associated with B and C class flares and studied the correlations for them  
53 separately. In this case, correlation coefficient for the flare-CME relationship is found to be  
54  
55  
56  
57  
58  
59  
60  
61  
62  
63  
64  
65

below  $R = 0.3$  in both the cycles. In this way, it is confirmed that the flare-CME relationship is much poorer for B+C class events than for M+X class events.

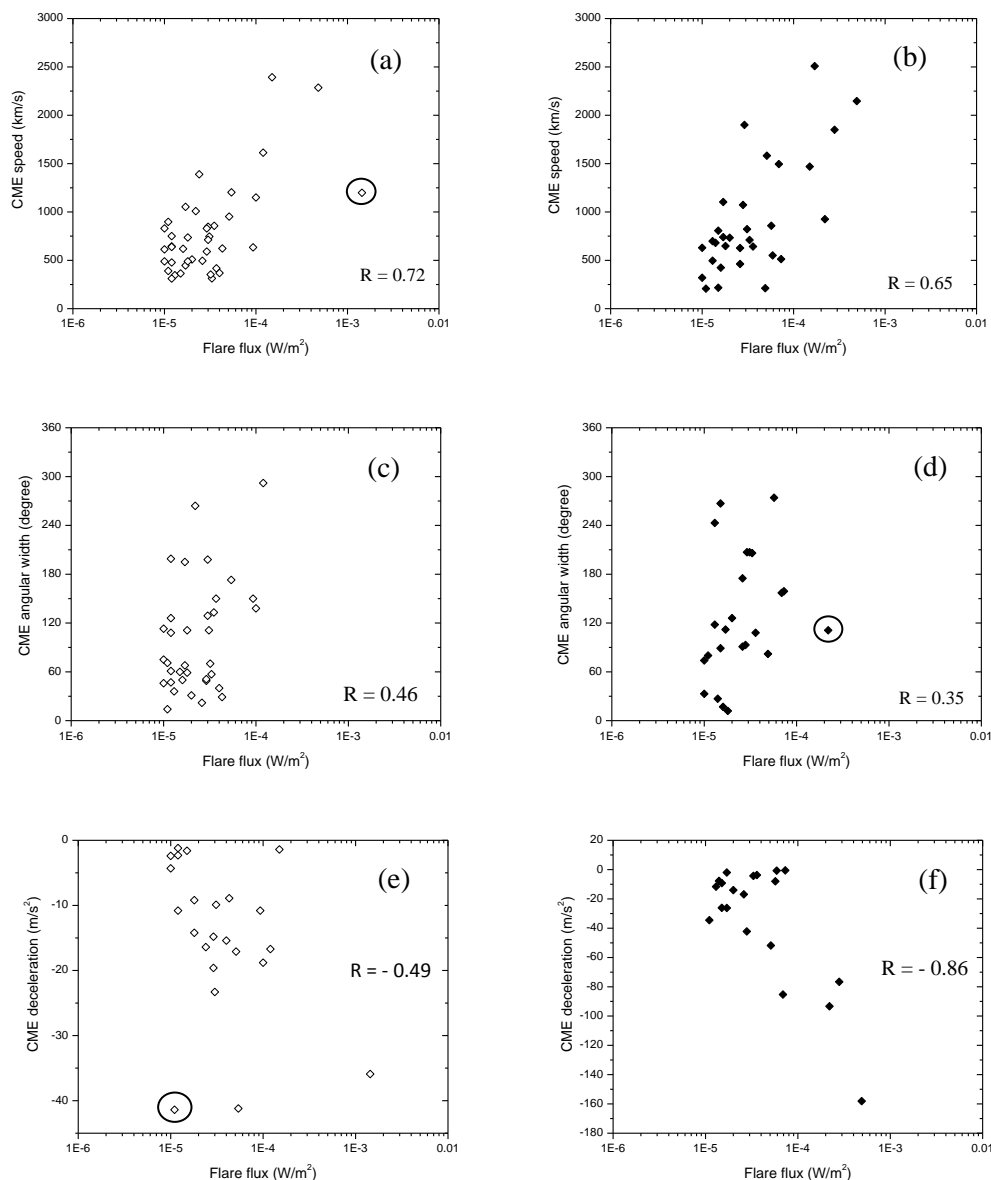


Fig. 5. Similar to Fig. 4, but for M and X flare class events only. 23<sup>rd</sup> solar cycle (left column) and 24<sup>th</sup> solar cycle (right column). The outlier point is not included in the correlation in (a) and (d) and it is indicated by the encircled symbol. If the outlier events in Fig. 5a, 5d and 5e would be included, the correlation coefficients would be  $R = 0.37$ ,  $R = 0.10$  and  $R = -0.39$ .

In Table 2, third and fifth columns give the statistical significance of flare-CME correlations (the P - value, based on the t-test), calculated utilizing the number of events (N) and correlation coefficient R. If  $P \geq 0.05$  (or  $P \geq 5\%$ ), the correlation coefficient does not significantly differ from zero. It turns out that most of the flare-CME correlations are significant for correlation co-efficient larger than  $\sim 0.3$ . For lower correlation coefficient values, flare-CME correlations are not significant.

### 3.2.3. Relationship between flare duration and CME parameters

For all the limb events, we analysed the relationship between the flare duration and rising time and the CME speed and angular width for both solar cycles. We found that there is only a very weak relation between these parameters (figures are not shown here). However, we found some differences in these relationships for the set of M+X class associated events (Fig. 6). These plots show better relations for Solar Cycle 23 ( $R = 0.3$  to  $0.5$ ) than for the cycle 24 ( $R = 0.06$  to  $0.3$ ). For the considered samples, the correlation coefficients and their significance are compared in Table 2. Inspecting the table, one finds that for the set of M+X class events the correlations in Solar Cycle 24 is not significant, whereas in cycle 23 the correlations are statistically significant.

Additionally, we checked the coefficients using square-law relationship of the form  $y=ax^2+bx+c$ , for the plots in Fig.6 and found a slight increase in the correlation coefficients for several relations (see the bracketed values in Table 2). The square-law relationship indicates that, as the flare duration grows to a certain value, the CME velocity and angular width decrease, but then, for larger flare durations, these CME characteristics start to increase with the duration. This approximation shows that the relationship between CME parameters and flare duration in 23<sup>rd</sup> solar cycle ( $R > 50\%$ ) is better than that in 24<sup>th</sup> solar cycle ( $R < 30\%$ ). The correlations with the rise time are similar for both cycles.

Table 2: Comparison of correlation coefficient of determination using linear (quadratic) fitting in Solar Cycles 23 and 24.

For all the events	Cycle 23		Cycle 24	
	Correlation coefficient	Correlation significance	Correlation coefficient	Correlation significance
Flare flux vs CME speed	0.60	~0.00	0.68	~0.00
Flare flux vs CME angular width	0.50	~0.00	0.55	~0.00
Flare flux vs CME deceleration	-0.18	<b>0.80</b>	<b>-0.82</b>	~0.00
Flare duration vs CME angular width	0.31	~0.00	0.22	0.04
Flare duration vs CME speed	0.45	~0.00	0.29	~0.00
Flare rising time vs CME angular width	0.29	~0.00	0.03	<b>0.79</b>
Flare rising time vs CME speed	0.46	~0.00	0.27	~0.00
<b>For M and X class events</b>				
Flare flux vs CME speed	0.72	~0.00	0.65	~0.00
Flare flux vs CME angular width	0.46	~0.00	0.35	0.09
Flare flux vs CME deceleration	-0.49	0.06	<b>-0.86</b>	~0.00
Flare duration vs CME angular width	0.39 (0.52)	0.02	0.06 (0.17)	<b>0.78</b>
Flare duration vs CME speed	0.49 (0.55)	~0.00	0.24 (0.27)	0.19
Flare rising time vs CME angular width	0.27 (0.27)	0.12	0.09 (0.30)	<b>0.68</b>
Flare rising time vs CME speed	0.48 (0.48)	~0.00	0.29 (0.47)	0.11

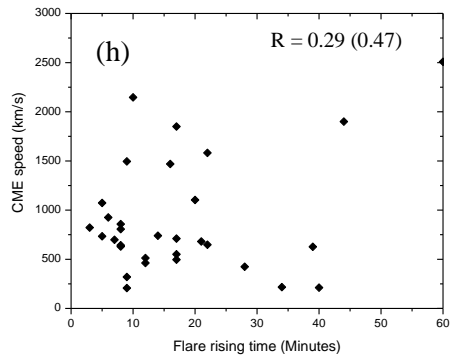
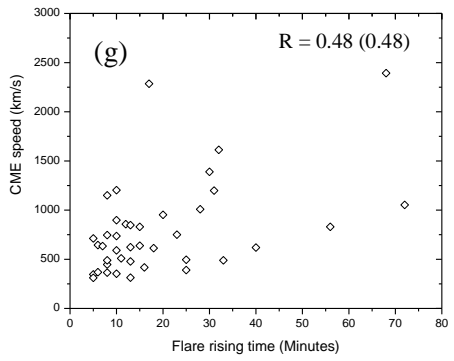
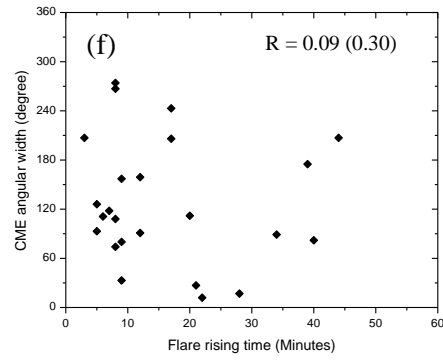
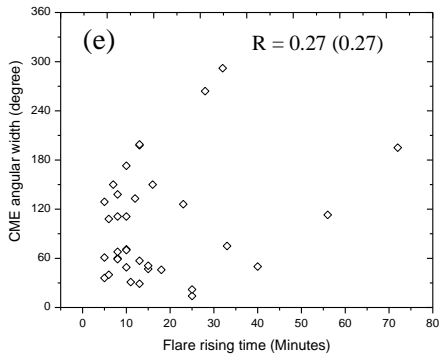
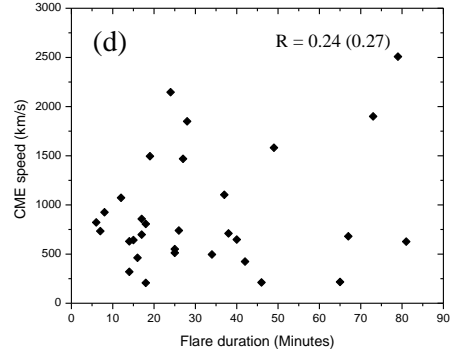
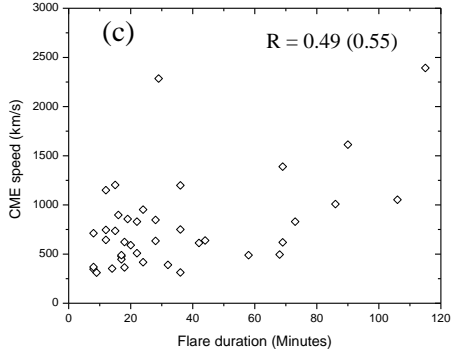
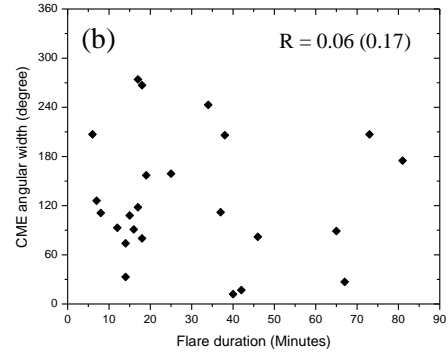
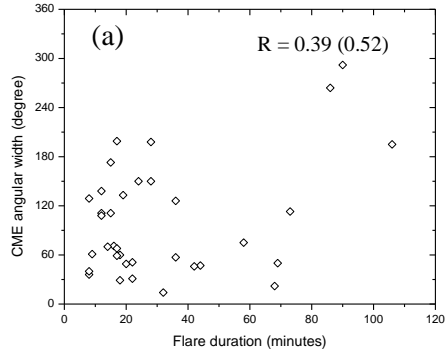


Fig. 6. CME - flare relation for M+X flare class events only, 23<sup>rd</sup> solar cycle (left column) and 24<sup>th</sup> solar cycle (right column). Correlation coefficient values for linear (quadratic) fitting are given in the plots.

1  
2  
3  
4  
5  
6  
7  
8  
9  
10  
11  
12  
13  
14  
15  
16  
17  
18  
19  
20  
21  
22  
23  
24  
25  
26  
27  
28  
29  
30  
31  
32  
33  
34  
35  
36  
37  
38  
39  
40  
41  
42  
43  
44  
45  
46  
47  
48  
49  
50  
51  
52  
53  
54  
55  
56  
57  
58  
59  
60  
61  
62  
63  
64  
65

Also, we recalculated the flare end time using flare peak flux divided by Euler number (2.718). We found the flare end time using this method and the resultant flare duration values are increased. For 23rd and 24th Solar Cycle events, we obtained correlation coefficient between flare duration calculated with divisor 2.718 and CME speed/angular width as  $R=0.37/0.18$  and  $R=0.25/0.06$ , respectively. From the results we concluded that there is a slightly better relationship between flare duration and CME speed/angular width for the 23<sup>rd</sup> Solar Cycle (plots are not shown here).

## 4. Conclusion

We investigated the properties of CMEs and flares and flare-CME relationship during the rising phase of Solar Cycles 23 [1996 May - 2002 June] and 24 [2008 December - 2014 December] using a set of events obtained from online CME catalogue observed by SOHO/LASCO and X-ray flares observed by GOES. We selected a sample of limb events (longitude =  $70^\circ - 85^\circ$ ) using the flare location data. Totally, 129 flare-CME pairs from Solar Cycle 23 and 92 flare-CME pairs from Solar Cycle 24 are selected using certain temporal and spatial criteria. The CME properties (speed, angular width and deceleration) and flares (rising time and duration), and relationships between them have been analysed, to check for possible differences between the two cycles. Next, we repeated the analysis considering only the events associated with M+X class flares (40 and 31 flare-CME pairs in cycles 23 and 24, respectively). The results we summarize as follows.

(i) The mean values of all CME and flare parameters are nearly same in the two cycles, except for the angular width of CMEs associated with M+X flares (Table 1).

(ii) The relationship between the flare SXR flux and CME deceleration is apparently different in the two cycles, but when we removed the X-class flare from the list of events, the correlation become weaker and similar for both cycles;

(iii) A difference in the relationship between flare SXR flux and CME deceleration might be also attributed to a larger number of X-class flares in Solar Cycle 24;

(iv) When the events associated with M+X class flares are considered separately, correlations between flare rise time and duration and the CME parameters are slightly better for cycle 23 than cycle 24 (Table 2). The above results can be attributed to the anomalous expansion of CMEs in the 24<sup>th</sup> solar cycle (Gopalswamy et al., 2014).

## Acknowledgement

1 The CME catalogue we have used is generated and maintained by the CDAW Data  
2 Centre by NASA and The Catholic University of America in cooperation with the Naval  
3 Research Laboratory and NASA. SOHO is a project of international cooperation between  
4 ESA and NASA. M. S. would like to thank Dr. P. K. Manoharan, Dr. S. Prasanna  
5 Subramanian, Radio Astronomy Centre, NCRA, TIFR, Ooty, Tamilnadu, India and  
6 Dr. Bhuwan Joshi, Reader, Udaipur Solar Observatory, PRL, Udaipur, Rajasthan, India. The  
7 grant to A.S. from University Grants Commission, Govt. of India, through major research  
8 project F. No. 42-845/2013 (SR) is kindly acknowledged. BV acknowledges financial  
9 support by Croatian Science Foundation under the project 6212 “Solar and Stellar  
10 Variability”.

## References:

- 22 • Andrews, M. D., Howard, T. S., 2001. A two type classification of LASCO coronal mass  
23 ejection. *Space Sci. Rev.* 95, 147-163.
- 24 • Bak-Steslicka, U., Kolomanski, S., Mrozek, T., 2013. Coronal mass ejection associated  
25 with slow long duration flares. *Solar Phy.* 283, 505-517.
- 26 • Christe, S., Hannah, I. G., Krucker, S., McTiernan, J., Lin, R. P., 2008. RHESSI micro-  
27 flare statistics. I. Flare-finding and frequency distributions. *Astrophys. J.* 677, 1385-1394.
- 28 • Compagnino, A., Romano, P., Zuccarello, F., 2017. A statistical study of CME properties  
29 and of the correlation between flares and CMEs over Solar Cycles 23 and 24. *Solar Phy.*  
30 292, 19.
- 31 • Conway, A. J., Matthews, S. A., 2003. The apparent longitude distribution of solar flares.  
32 *Astron. Astrophys.* 401, 1151-1157.
- 33 • Gopalswamy, N., Yashiro, S., Kaiser, M. L., Howard, R. A., Bougeret, J. L., 2001. Radio  
34 signatures of coronal mass ejection interaction: CME cannibalism?. *Astrophys. J.* 548,  
35 L91-L94.
- 36 • Gopalswamy, N., Yashiro, S., Michalek, G., Stenborg, G., Vourlidas, A., Freeland, S.,  
37 Howard, R., 2009. The SOHO/LASCO CME catalogue. *Earth, Moon, and Planets*, 104,  
38 295-313.
- 39 • Gopalswamy, N., Akiyama, S., Yashiro, S., Xie, H., Makela, P., Michalek, G., 2014.  
40 Anomalous expansion of coronal mass ejections during solar cycle 24 and its space  
41 weather implications. *Geophys. Res. Lett.* 41, 2673-2680.



- 1 • Gopalswamy, N., Xie, H., Akiyama, S., Makela, P., Yashiro, S., Michalek, G., 2015a.  
2 The peculiar behaviour of halo coronal mass ejection in solar cycle 24. *Astrophys. J.* 804,  
3 L23-L28.
- 4 • Gopalswamy, N., Yashiro, S., Xie, H., Akiyama, S., Makela, P., 2015b. Properties and  
5 geo-effectiveness of magnetic clouds during solar cycle 23 and 24. *J. Geophys. Res.* 120,  
6 9221-9245.
- 7 • Gosling, J. T., Hildner, E., MacQueen, R. M., Munro, R. H., Poland, A. I., Ross, C. L.,  
8 1976. The speed of coronal mass ejection events. *Solar Phys.* 48, 389-397.
- 9 • Harrison, R. A., 1995. The nature of solar flares associated with coronal mass ejection.  
10 *Astron. Astrophys.* 304, 585-594.
- 11 • Hundhausen, A. J., 1997. In *Coronal Mass Ejections. Geophysical Monograph 99*, ed. N.  
12 Crooker, et al. (Washington, DC: AGU), 1.
- 13 • Jain, R., Aggarwal, M., Kulkarni, P., 2010. Relationship between CME dynamics and  
14 solar flare plasma. *Research in Astronomy and Astrophysics.* 10, 473-483.
- 15 • Joshi, B., Manoharan, P. K., Veronig, A. M., Pant, P., Pandey, K. 2007. Multi-  
16 wavelength signatures of magnetic reconnection of a flare associated coronal mass  
17 ejections. *Sol. Phys.* 242, 143.
- 18 • Joshi, B., Veronig, A., Cho, K.-S., Bong, S. C., Somov, B. V., Moon, Y. J., Lee, J.,  
19 Manoharan, P.K., Kim, Y. H. Magnetic reconnection during the two phase evolution of a  
20 solar eruptive flare. 2009, *Astrophys. J.* 706, 1438.
- 21 • Joshi, B., Veronig, A. M., Lee, J., Cho, K.S. Pre-flare activity and magnetic reconnection  
22 during the evolutionary stages of energy release in a solar eruptive flare. 2011, *Astrophys.*  
23 *J.* 743, 195.
- 24 • Joshi, B., Veronig, A., Manoharan, P. K., Somov, B. V. 2012, in *Astrophysics and Space*  
25 *Science Proceedings, Vol. 33, Multi-scale Dynamical Processes in Space and*  
26 *Astrophysical Plasmas*, ed. M. P. Leubner Z. V (Springer-Verlag Berlin Heidelberg), 29.
- 27 • Kahler, S. W., 1992. Solar flares and coronal mass ejections. *Annual review of astronomy*  
28 *and astrophysics.* 30, 113-141.
- 29 • Lin, R. P., Dennis, B. R., Hurford, G. J., Smith, D. M., et al. 2002. The Reuven Ramaty  
30 High-Energy Solar Spectroscopic Imager (RHESSI). *Solar Phys.* 210, 3-32.
- 31 • MacQueen, R. M., Fisher, R. R., 1983. The kinematics of solar inner coronal transients.  
32 *Solar Phys.* 89, 89-102.
- 33 • Mahrous, A., Shaltout, M., Beheary, M. M., Mawad, R., Youssef, M., 2009. CME-flare  
34 association during the 23<sup>rd</sup> solar cycle. *Adv. Space Res.*, 43, 1032-1035.

- 1 • Manoharan, P.K., Gopalswamy, N., Yashiro, S., Lara, A., Michalek, G., Howard, R.A.,  
2 2004. Influence of coronal mass ejection on propagation of interplanetary Shocks. *J.*  
3 *Geophys. Res.* 109, A06109.
- 4 • Manoharan, P.K., 2006. Evolution of coronal mass ejections in the inner heliosphere: a  
5 study using white light and scintillation images. *Sol. Phys.* 235, 345–368.
- 6 • Maricic, D., Vrsnak, B., Stanger, A. L., Veronig, A. M., Temmer, Rosa, D., 2007.  
7 Acceleration Phase of Coronal Mass Ejections: II. Synchronization of the Energy Release  
8 in the Associated Flare. *Sol. Phys.* 241, 99–112.
- 9 • Munro, R. H., Gosling, J. T., Hinldner, E., MacQueen, R. M., Poland, A. I., Ross, C. L.,  
10 1979. The association of coronal mass ejection transients with other forms of solar  
11 activity. *Solar Phys.*, 61, 201-215.
- 12 • Moon, Y. J., Choe, G. S., Wang, H., Park, Y. D., Gopalswamy, N., Yang, G., Yashiro, S.,  
13 , 2002. A statistical study of two classes of coronal mass ejections. *Astrophys. J.*, 581,  
14 694-702.
- 15 • Prakash, O., Shanmugaraju, A., Michalek, G., Umapathy, S., 2014. Geo-effectiveness and  
16 flare properties of radio- loud CMEs. *Astrophys. Space Sci.*, 350, 33-45.
- 17 • Prasanna Subramanian, S., Shanmugaraju, A., 2016. Study of intensive solar flares in the  
18 rise phase of solar cycle 23 and 24 and other activities. *Astrophys. Space Sci.*, 361, 78-86.
- 19 • Salas-Matamoros, C., Klein, K. L., 2015. On the statistical relationship between CME  
20 speed and soft X-ray flux and fluence of the associated flare. *Solar Phys.* 290, 1337-1353.
- 21 • Shanmugaraju, A., Moon, Y. J., Dryer, M., Umapathy, S., 2003. Statistical characteristics  
22 of CMEs and flares associated with solar type II radio bursts. *Solar Phys.* 217, 301-317.
- 23 • Shanmugaraju, A., Moon, Y. J., Vrsnak, B., 2011. Correlation between CME and flare  
24 parameters (with and without type II burst). *Solar Phys.* 270, 273-284.
- 25 • Shanmugaraju, A., Bendict Lawrance, M., 2015. Halo coronal mass ejections and their  
26 relation to DH type-II radio bursts. *Solar Phys.* 290, 2963-2973.
- 27 • Sheeley, N. R., Walters, H., Wang, Y.-M., Howard, R. A., 1999. Continuous tracking of  
28 coronal outflows: Two kind of coronal mass ejections. *J. Geophys. Res.* 104, 24739-  
29 24768.
- 30 • Vrsnak, B., Maricic, D., Stanger, A. L., Veronig, A., 2004. Coronal mass ejection of 15  
31 May 2001: II. Coupling of CME acceleration and flare energy release. *Solar Phys.* 225,  
32 355-378.
- 33 • Vrsnak, B., Sudar, D., Ruzdjak, D., 2005. The CME - flare relationship: Are there really  
34 two types of CMEs?. *Astron. Astrophys.* 435, 1149-1157.

- Vrsnak, B., Maricic, D., Stanger, A. L., Veronig, A. M., Temmer, M., and Rosa, D., 2007. Acceleration Phase of Coronal Mass Ejections: I. Temporal and Spatial Scales. *Sol. Phys.* 241, 85–98.
- Vrsnak, B., Zic, T., Falkenberg, T. V., Mostl, C., Vennerstrom, S., Vrbanec, D., 2010. The role of aerodynamic drag in propagation of interplanetary coronal mass ejection. *Astron. Astrophys.* 512, A43.
- Youssef, M., 2012. On the relation between CMEs and solar flares, *J. Astronomy and Geophysics*, 1,172-178.
- Yashiro, S., Gopalswamy, N., 2009. Statistical relationship between solar flares and coronal mass ejections. *Proceedings of the International Astronomical Union, IAU Symposium*, 257, 233-243.
- Zhang, J., Dere, K. P., Howard, R. A., Kundu, M. R., White, S. M., 2001. On the temporal relationship between coronal mass ejection and flares. *Astrophys. J.* 559, 452-462.
- Zhang, J., Dere, K. P., 2006. A statistical study of main and residual acceleration of coronal mass ejections. *Astrophys. J.*, 649, 1100-1109.